Hindawi Publishing Corporation
Mathematical Problems in Engineering
Volume 2015, Article ID 714136, 10 pages
http://dx.doi.org/10.1155/2015/714136

Research Article

Variational Approach for Resolving the Flow of Generalized Newtonian Fluids in Circular Pipes and Plane Slits

Taha Sochi

Department of Physics & Astronomy, University College London, Gower Street, London WC1E 6BT, UK

Correspondence should be addressed to Taha Sochi; t.sochi@ucl.ac.uk

Received 22 March 2015; Accepted 8 June 2015

Academic Editor: Yannis Dimakopoulos

We use a generic and general variational method to obtain solutions to the flow of generalized Newtonian fluids through circular pipes and plane slits. The new method is not based on the use of the Euler-Lagrange variational principle and hence it is totally independent of our previous approach which is based on this principle. Instead, the method applies a very generic and general optimization approach which can be justified by the Dirichlet principle although this is not the only possible theoretical justification. The results that were obtained from the new method using nine types of fluid are in total agreement, within certain restrictions, with the results obtained from the traditional methods of fluid mechanics as well as the results obtained from the previous variational approach. In addition to being a useful method in its own for resolving the flow field in circular pipes and plane slits, the new variational method lends more support to the old variational method as well as for the use of variational principles in general to resolve the flow of generalized Newtonian fluids and obtain all the quantities of the flow field which include shear stress, local viscosity, rate of strain, speed profile, and volumetric flow rate.

1. Introduction

The flow through circular pipes and plane slits has many applications in physical and biological sciences and engineering and hence it has been investigated in the past by many researchers (e.g., [1–13]) using various methods of fluid dynamics. Recently we proposed the use of Euler-Lagrange variational principle [14] to resolve the flow of generalized Newtonian fluids through circular pipes. The method is based on minimizing the total stress in the flow conduit in the sense of minimizing the stress profile in the velocity-varying dimension. This attempt was later expanded and supported by other investigations [15–17] where the method was successfully applied to more types of fluid and another type of geometry, namely, the plane slit conduit.

Despite the success of this method in describing the flow of several fluid models and conduit types, it has not been proven in general by a formal mathematical argument that justifies the universal applicability of the variational method and the principle on which it relies. Certain mathematical technicalities may also be disputed and hence it is desirable to fortify the method by a more generic and general variational approach that is more safe from such disputes and pitfalls. The present investigation tries to do so by using a very basic and general variational approach where the flow field in the conduit is resolved through the application of a generic optimization technique to a stress functional. The theoretical justification of this functional can be obtained from the Dirichlet principle although it can also be justified by other theoretical foundations based on purely physical arguments.

The plan for this paper is that in Section 2 we present a general description of the proposed method and its theoretical background. This is followed in Section 3 by discussing practical issues about the implementation of this method and the presentation of sample results that were obtained from this method with comparison to similar results obtained from the previous methods which include the classical methods of fluid mechanics and the former variational approach. The paper is finalized in Section 4 with general discussions and summarization of the main achievements of the present study. As a matter of convenience, we label the former variational method which is based on the Euler-Lagrange

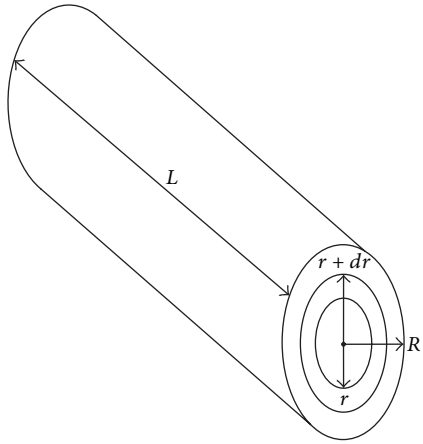

Figure 1: A schematic of the circular pipe geometry used in this investigation.

principle with EL and the new variational method which is based on the Dirichlet principle with DM.

2. Method

We first state our assumptions about the flow, fluid, and conduit which are adopted in the present study. We assume a laminar, isothermal, incompressible, steady, pressure-driven, fully developed flow of a time-independent, purely viscous fluid that can be described by the generalized Newtonian fluid model; that is,

$$\tau = \mu\gamma, \tag{1}$$

where the viscosity, μ, and stress, τ, depend only on the contemporary rate of strain, γ, and hence the fluid has no memory of its deformation past. In this formulation we ignore all non-deformation-related dependencies of the viscosity and stress due to other physical factors like temperature and pressure. In fact we consider only the shearing effects since the effects of other forms of deformation, such as extensional, are presumed insignificant which is well justified for the presumed state of flow, fluid, and conduit. Edge effects at the entry and exit of the conduit, as well as external body forces, are also regarded negligible.

Concerning the conduit, we use circular pipe and plane slit geometries, which are depicted in Figures 1 and 2, where the pipe is assumed straight with a cross section that is uniform in shape and size while the slit is assumed straight long and thin with a uniform cross section. In both cases we assume rigid mechanical characteristics of the conduit wall as opposite to being deformable such as having elastic or viscoelastic mechanical properties. It is also assumed that the slit is positioned symmetrically in its thickness dimension, z, with respect to the plane $z = 0$ as depicted in Figure 2.

Regarding the boundary conditions, we assume no slip at the conduit wall, where the fluid interfaces the solid [18], with the flow speed profile having a stationary derivative point at the symmetry center line of the pipe and symmetry center plane of the slit which means zero stress and rate of strain at

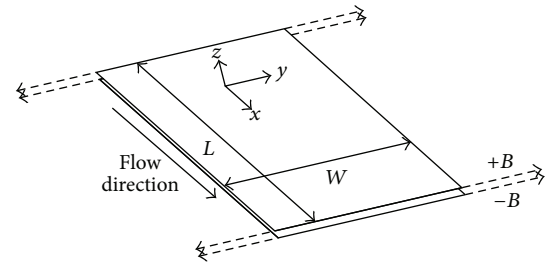

Figure 2: A schematic of the plane slit geometry used in this investigation.

these loci. As for the viscoplastic fluids, this stationary region expands to include all the points at the forefront of the flow profile whose stress falls below the yield stress, as will be discussed further in the coming sections.

Now, for the generalized Newtonian fluids that satisfy the above assumptions, the momentum equation in one dimension is reduced to

$$\frac{d\tau}{ds} = G, \tag{2}$$

where s is a spatial coordinate that represents r for pipes and z for slits and G is a constant. If we differentiate the last equation with respect to s we get

$$\frac{d^2\tau}{ds^2} = 0 \tag{3}$$

which is a one-variable Laplace equation in one dimension. According to the Dirichlet principle, the solution of this equation is a minimizer of the following functional and vice versa:

$$D = \int_\Omega \left| \left(\frac{d\tau}{ds} \right)^2 ds \right|, \tag{4}$$

where D is the Dirichlet functional and Ω is a spatial domain in this formulation. On using (2), substituting, and simplifying, the functional can be reduced to

$$D = |G| \int_T d\tau, \tag{5}$$

where T is the new domain in this formulation. The last equation demonstrates that the solution of this problem is a minimizer (and vice versa) of the total stress in the sense that has been given previously and hence it establishes the foundation of our former variational approach, EL, which is based on the use of the Euler-Lagrange principle. It can also provide a theoretical foundation for new method or methods.

Apart from its theoretical aspects, the Dirichlet principle can be used practically as a basis for another variational method, DM, that can be employed to obtain flow solutions and verify the solutions obtained by other methods including the EL method. The DM method in practical terms is based on finding the shear stress solution in conduits by minimizing the above functional. This functional is discretized and minimized numerically using an optimization algorithm subject

Table 1: The constitutive relations for the nine fluid models used in this investigation. The meaning of the symbols is given in Nomenclature.

Model	Constitutive relation
Newtonian	$\tau = \mu_o \gamma$
Power Law	$\tau = k\gamma^n$
Ellis	$\mu = \mu_e \left[1 + \left(\frac{\tau}{\tau_h}\right)^{\alpha-1}\right]^{-1}$
Ree-Eyring	$\tau = \tau_c \operatorname{arcsinh}\left(\frac{\mu_r \gamma}{\tau_c}\right)$
Carreau	$\mu = \mu_i + (\mu_0 - \mu_i)\left(1 + \lambda^2\gamma^2\right)^{(n-1)/2}$
Cross	$\mu = \mu_i + \frac{\mu_0 - \mu_i}{1 + \lambda^m \gamma^m}$
Bingham	$\tau = C'\gamma + \tau_0$
Herschel-Bulkley	$\tau = C\gamma^n + \tau_0$
Casson	$\tau^{1/2} = (K\gamma)^{1/2} + \tau_0^{1/2}$

to the boundary conditions at the conduit wall and conduit center. For pipes these boundary conditions are, respectively,

$$\tau_w \equiv \tau_R = \frac{R\Delta p}{2L}, \qquad \tau_m = 0 \tag{6}$$

while for slits they are

$$\tau_w \equiv \tau_B = \frac{B\Delta p}{L}, \qquad \tau_m = 0, \tag{7}$$

where τ_w is the shear stress at the conduit wall which is equivalent to τ_R for pipes and to τ_B for slits, τ_m is the stress at the conduit center line or plane, R is the pipe radius, B is the slit half thickness, and L is the conduit length across which a pressure drop Δp is exerted.

The numerically obtained solution, $\tau(s)$, is then used in conjunction with the rheological constitutive relations, as given in Table 1 for the models considered in this study, applied to the generalized Newtonian fluid equation to find $\gamma(s)$ either explicitly or implicitly through the use of a simple numerical solver like a bisection solver. As for the viscoplastic fluids, a zero stress is applied to all the points at the forefront of the flow profile whose shear stress falls below the yield stress value during the optimization process. As indicated earlier, this is an extension to the second boundary condition at the conduit center to include a plane region in the forefront of the speed profile and hence it does not compromise the optimization condition and the underlying variational principle.

The obtained $\gamma(s)$ is then integrated numerically with respect to s to find the flow speed, $v(s)$, where the no-slip boundary condition at the conduit wall is used to provide an initial value, $v = 0$, that is incremented on moving inward from the conduit wall toward the conduit center during the integration process. This is followed by integrating $v(s)$ numerically with respect to the conduit cross-sectional area normal to the flow direction to obtain the volumetric flow rate. During these successive integration processes, the boundary conditions at the conduit wall and center, which are based on the zero speed and zero stress, respectively, are used.

In Table 1 the rheological constitutive relations for the nine fluid models which are employed in this study are presented, while in Tables 2 and 3 the analytical relations that correlate the flow rate, Q, to the applied pressure drop, Δp, for the flow in pipes and slits, respectively, are given. Most of these expressions can be found in the classic literature of rheology and fluid dynamics (e.g., [19, 20]) while the rest can be obtained with their derivation from [15–17]. Regarding the Carreau and Cross fluids, the "I" factors, which are included in their Q expressions and represent definite integral expressions, are given by

$$I_{\mathrm{p,Ca}} = \frac{\delta^3\left[3\lambda^4\left(3n'^2 + 5n' + 2\right)\gamma_R^4 - 3n'\lambda^2\gamma_R^2 + 2\right]\left(1 + \lambda^2\gamma_R^2\right)^{3n'/2}}{3\lambda^4\left(9n'^2 + 18n' + 8\right)}$$

$$+ \frac{\mu_i\delta^2\left[\lambda^4\left(2n'^2 + 5n' + 3\right)\gamma_R^4 - n'\lambda^2\gamma_R^2 + 1\right]\left(1 + \lambda^2\gamma_R^2\right)^{n'}}{2\lambda^4\left(n' + 1\right)\left(n' + 2\right)}$$

$$+ \frac{\mu_i^2\delta\left[\lambda^4\left(n'^2 + 5n' + 6\right)\gamma_R^4 - n'\lambda^2\gamma_R^2 + 2\right]\left(1 + \lambda^2\gamma_R^2\right)^{n'/2}}{\lambda^4\left(n' + 2\right)\left(n' + 4\right)} + \frac{\mu_i^3\gamma_R^4}{4}$$

$$- \left(\frac{2\delta^3}{3\lambda^4\left(9n'^2 + 18n' + 8\right)} + \frac{\mu_i\delta^2}{2\lambda^4\left(n' + 1\right)\left(n' + 2\right)} + \frac{2\mu_i^2\delta}{\lambda^4\left(n' + 2\right)\left(n' + 4\right)}\right)$$

$$I_{\mathrm{p,Cr}} = \frac{\left\{2\delta^3\left[-m\left(2f^2 + 5f + 3\right) + 4g^2 + 2m^2\right] + 12m\delta^2\mu_i g\left(m - g\right) + 12m^2\delta\mu_i^2 g^2 + 3m^2\mu_i^3 g^3\right\}\gamma_R^4}{12m^2 g^3}$$

$$
\begin{aligned}
&- \frac{\left\{\delta^3\left(m^2-6m+8\right)+3m\delta^2\mu_i\left(m-4\right)+3m^2\delta\mu_i^2\right\}\ {}_2F_1\left(1,4/m;\left(m+4\right)/m;-f\right)\gamma_R^4}{12m^2}\\
I_{\mathrm{s,Ca}} &= \frac{n'\delta^2\gamma_B\left[\ {}_2F_1\left(1/2,1-n';3/2;-\lambda^2\gamma_B^2\right)-\ {}_2F_1\left(1/2,-n';3/2;-\lambda^2\gamma_B^2\right)\right]}{\lambda^2}+\frac{\left(1+n'\right)\delta^2\gamma_B^3\,{}_2F_1\left(3/2,-n';5/2;-\lambda^2\gamma_B^2\right)}{3}\\
&+ \frac{n'\delta\mu_i\gamma_B\left[\ {}_2F_1\left(1/2,1-n'/2;3/2;-\lambda^2\gamma_B^2\right)-\ {}_2F_1\left(1/2,-n'/2;3/2;-\lambda^2\gamma_B^2\right)\right]}{\lambda^2}\\
&+ \frac{\left(2+n'\right)\delta\mu_i\gamma_B^3\,{}_2F_1\left(3/2,-n'/2;5/2;-\lambda^2\gamma_B^2\right)+\mu_i^2\gamma_B^3}{3},\\
I_{\mathrm{s,Cr}} &= \frac{\left[3\delta^2\left(m-g\right)-\left\{\delta^2\left(m-3\right)+2m\delta\mu_i\right\}g^2\ {}_2F_1\left(1,3/m;1+3/m;-f\right)+6m\delta\mu_i g+2m\mu_i^2g^2\right]\gamma_B^3}{6mg^2},
\end{aligned}
\tag{8}
$$

where, in these expressions,

$$
\begin{aligned}
\delta &= \left(\mu_0-\mu_i\right),\\
n' &= \left(n-1\right),\\
f &= \lambda^m\gamma_w^m,\\
g &= 1+f,
\end{aligned}
\tag{9}
$$

and ${}_2F_1$ is the hypergeometric function of the given arguments with its real part being used in the evaluation of I factors. Moreover,

$$
\begin{aligned}
\mu_R\gamma_R &= \tau_R,\\
\mu_B\gamma_B &= \tau_B,
\end{aligned}
\tag{10}
$$

where τ_R and τ_B are given by (6) and (7), respectively, with γ_R and γ_B being obtained numerically from the above implicit relations, as explained in [17].

3. Implementation and Results

The optimization method, as described in the last section, was implemented in a computer code using five numerical optimization algorithms: three deterministic which are Conjugate Gradient, Quasi-Newton, and Nelder-Mead [21] and two stochastic which are the stochastic global algorithm of Boender et al. [22] (see also http://jblevins.org/mirror/amiller/global.txt web page) and a generic simulated annealing algorithm [23]. These five algorithms produce similar solutions with different levels of accuracy and convergence rate. The sample results presented in this paper are obtained mostly from the stochastic global algorithm which is overwhelmingly the most accurate and reliable one. In addition, standard numerical integration and bisection solution techniques, as well as standard algorithms for evaluating complicated functions like the hypergeometric function, were employed.

The newly proposed variational method was then employed to obtain solutions for the flow of nine types of fluid through pipes and slits. The nine types of fluid are as follows: Newtonian, Power Law, Ellis, Ree-Eyring, Carreau, Cross, Bingham, Herschel-Bulkley, and Casson. The results obtained from the new method using wide ranges of fluid and conduit parameters were thoroughly compared to the results obtained from the traditional methods of fluid mechanics and the former variational method.

In all the investigated cases the three methods produced very similar results within acceptable error margins. One exception is the Ellis model for which EL has not been formulated and implemented. Another exception is the viscoplastic fluids where the EL method differs significantly when the yield stress value is high. This is justified by the fact that the EL method was formulated and implemented for the nonviscoplastic fluids specifically and hence, as we demonstrated in our previous investigations [14–16], it is just an approximation for the viscoplastic fluids which is a good one only when the yield stress value is low. However, we believe that even the EL method can be reformulated and reimplemented to include viscoplastic fluids, and hence it can produce similar results to the other methods even for the high yield stress fluids, although we did not make any effort in the current study to do so.

A representative sample of these results obtained from the three methods is presented in Figures 3, 4, 5, and 6 where the fluid and conduit parameters of these examples are given in Tables 4 and 5. In these figures, the analytical solution is represented by the solid line while the solutions from the two variational methods are represented by the circles. The exception, as indicated earlier, is the Ellis and viscoplastic fluids where the circles represent only the DM method. The reason for combining the solutions of the two variational methods in a single representation is that they produce very similar results and hence there is no point in plotting them separately.

As seen in these examples, the two variational solutions agree very well with the analytical solutions. The minor departure in some cases between the two variational methods on one hand and the analytical on the other is mainly due to the nature of the variational methods as they heavily rely on

Table 2: The volumetric flow rate, Q, for the pipe flow of the nine fluid models used in this investigation. The symbols are given in Nomenclature.

Model	Q
Newtonian	$\dfrac{\pi R^4 \Delta p}{8 L \mu_o}$
Power Law	$\dfrac{\pi R^4}{8L} \sqrt[n]{\dfrac{\Delta p}{k}} \left(\dfrac{4n}{3n+1}\right) \left(\dfrac{2L}{R}\right)^{1-1/n}$
Ellis	$\dfrac{\pi R^3 \tau_R}{4\mu_e} \left[1 + \dfrac{4}{\alpha+3} \left(\dfrac{\tau_R}{\tau_h}\right)^{\alpha-1}\right]$
Ree-Eyring	$\dfrac{\pi R^3 \tau_c}{\tau_R^3 \mu_r} \left[\left(\tau_c \tau_R^2 + 2\tau_c^3\right) \cosh\left(\dfrac{\tau_R}{\tau_c}\right) - 2\tau_c^2 \tau_R \sinh\left(\dfrac{\tau_R}{\tau_c}\right) - 2\tau_c^3\right]$
Carreau	$\dfrac{\pi R^3 I_{\mathrm{p,Ca}}}{\tau_R^3}$
Cross	$\dfrac{\pi R^3 I_{\mathrm{p,Cr}}}{\tau_R^3}$
Bingham	$\dfrac{\pi R^4 \Delta p}{8 L C'} \left[\dfrac{1}{3}\left(\dfrac{\tau_0}{\tau_R}\right)^4 - \dfrac{4}{3}\left(\dfrac{\tau_0}{\tau_R}\right) + 1\right]$
Herschel-Bulkley	$\dfrac{8\pi}{\sqrt[n]{C}} \left(\dfrac{L}{\Delta p}\right)^3 \left(\tau_R - \tau_0\right)^{1+1/n} \left[\dfrac{\left(\tau_R - \tau_0\right)^2}{3+1/n} + \dfrac{2\tau_0\left(\tau_R - \tau_0\right)}{2+1/n} + \dfrac{\tau_0^2}{1+1/n}\right]$
Casson	$\dfrac{\pi R^3}{\tau_R^3 K} \left(\dfrac{\tau_R^4}{4} - \dfrac{4\sqrt{\tau_0}\tau_R^{7/2}}{7} + \dfrac{\tau_0 \tau_R^3}{3}\right)$

Table 3: The volumetric flow rate, Q, for the slit flow of the nine fluid models used in this investigation. The symbols are given in Nomenclature.

Model	Q
Newtonian	$\dfrac{2WB^3 \Delta p}{3\mu_o L}$
Power Law	$\dfrac{2WB^2 n}{2n+1} \sqrt[n]{\dfrac{B\Delta p}{kL}}$
Ellis	$\dfrac{2WB^2}{\mu_e} \left[\dfrac{\tau_B}{3} + \dfrac{\tau_B^\alpha}{(\alpha+2)\,\tau_h^{\alpha-1}}\right]$
Ree-Eyring	$\dfrac{2W\tau_c^2}{\mu_r} \left(\dfrac{B}{\tau_B}\right)^2 \left[\tau_B \cosh\left(\dfrac{\tau_B}{\tau_c}\right) - \tau_c \sinh\left(\dfrac{\tau_B}{\tau_c}\right)\right]$
Carreau	$\dfrac{2WB^2 I_{\mathrm{s,Ca}}}{\tau_B^2}$
Cross	$\dfrac{2WB^2 I_{\mathrm{s,Cr}}}{\tau_B^2}$
Bingham	$\dfrac{2W}{C'} \left(\dfrac{B}{\tau_B}\right)^2 \left[\dfrac{\tau_B^3}{3} - \dfrac{\tau_0 \tau_B^2}{2} + \dfrac{\tau_0^3}{6}\right]$
Herschel-Bulkley	$\dfrac{2W}{\sqrt[n]{C}} \left(\dfrac{B}{\tau_B}\right)^2 \left[\dfrac{n\left(n\tau_0 + n\tau_B + \tau_B\right)\left(\tau_B - \tau_0\right)^{1+1/n}}{\left(2n^2 + 3n + 1\right)}\right]$
Casson	$\dfrac{2W}{K} \left(\dfrac{B}{\tau_B}\right)^2 \left[\dfrac{\tau_B^3}{3} - \dfrac{4\sqrt{\tau_0}\tau_B^{5/2}}{5} + \dfrac{\tau_0 \tau_B^2}{2} - \dfrac{\tau_0^3}{30}\right]$

numerical techniques, mainly bisection solvers and numerical integration, which is not the case with the analytical solutions since they are evaluated directly. As indicated above, unlike the EL approach which is a good approximation for the viscoplastic fluids only if their yield stress is low, the DM approach produces "exact" solutions, considering the numerical errors introduced by the heavy use of numerical techniques, even for the fluids with high yield stress.

4. Conclusions

In this paper we presented a variational approach for finding the flow solutions in one-dimensional flow that applies easily to circular pipes and plane slits. The method, which is demonstrated using nine types of fluid, can be employed to obtain all the required flow parameters which include shear stress, local viscosity, shear rate, speed profile, and volumetric flow rate. We also presented, through the application of the Dirichlet principle, a theoretical justification for the application of minimizing the total stress profile as a basis for our variational approaches including the EL method.

Thorough comparisons were made both to the analytical solutions obtained from the traditional methods of fluid dynamics and to the analytical or semianalytical solutions obtained from the EL method. In all cases, the three methods produced very close results where the differences can be explained by the numerical errors introduced by heavy use of numerical methods like numerical integration, bisection solvers, and numeric evaluation of complicated functions. The exception is the viscoplastic fluids for which the EL method cannot provide reliable solutions when the yield stress is high due to the particular formulation and implementation of this method which is restricted to nonviscoplastic fluids. The EL method also has not been formulated and

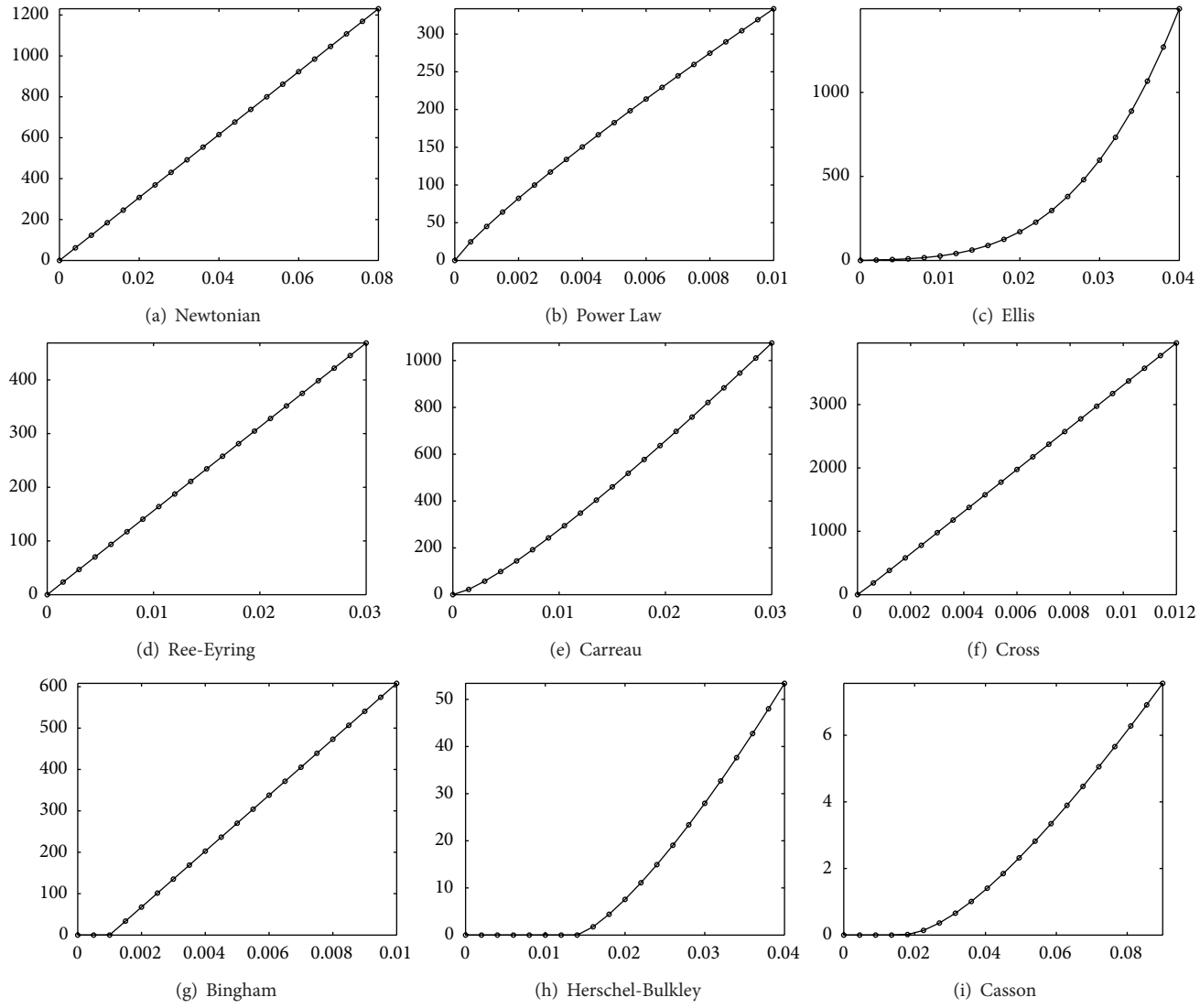

FIGURE 3: Comparing the analytical solution (solid line) to the variational solutions (circles) of γ in s^{-1} (vertical axis) versus r in m (horizontal axis) for the flow of the nine fluid models in pipes. The EL solutions are not represented for the Ellis and viscoplastic fluids. The pipe and fluid parameters are given in Table 4, where in all cases $\Delta p = 500$ Pa.

implemented in the past for the Ellis fluid and we did not make any effort to do so in the current study.

Apart from being useful on its own for resolving the flow field in the given conduits and obtaining all the required parameters, the proposed DM method adds more support to the previous EL approach, which is based on applying the Euler-Lagrange variational principle, as it confirms the results obtained from the EL method and provides a theoretical foundation for it. Although the new method may not be conceptually identical to the previous one, it should still lend support to the previous one not only because the two differently formulated variational methods produce similar results but also because they are both based on similar variational principles. From a procedural point of view, the two methods are equivalent because what is done in DM numerically is done in EL, as presented in our previous studies, either analytically or partly analytically and partly numerically. It has also been shown that the theoretical foundation of the DM method, represented by the Dirichlet principle, endorses the particular formulation of stress minimization which EL rests upon.

There is an obvious theoretical value of the new DM variational method which is more important than its practical value which may be insignificant for the investigated fluid types and conduit geometries due to the availability of the presented analytical and numerical flow solutions from other methods. If the proposed variational principle enjoys general applicability, which is yet to be established beyond the one-dimensional flow through pipes and slits, the method may also have a significant practical value for the flow systems which are more complicated than the flow systems in pipes and slits where the DM variational method may provide

Table 4: Fluid and pipe parameters for the examples of Figures 3 and 5. SI units apply to all dimensional quantities as given in Nomenclature.

Model	Fluid properties	R	L
Newtonian	$\mu_o = 0.025$	0.08	0.65
Power Law	$k = 0.033, n = 1.15$	0.01	0.095
Ellis	$\mu_e = 1.42, \tau_h = 15, \alpha = 3.3$	0.04	0.15
Ree-Eyring	$\mu_r = 0.02, \tau_c = 300$	0.03	0.8
Carreau	$\mu_0 = 0.1, \mu_i = 0.008, \lambda = 1.2, n = 0.65$	0.03	0.45
Cross	$\mu_0 = 0.15, \mu_i = 0.005, \lambda = 7.9, m = 0.8$	0.012	0.15
Bingham	$C' = 0.037, \tau_0 = 2.5$	0.01	0.1
Herschel-Bulkley	$C = 0.47, \tau_0 = 5.0, n = 0.75$	0.04	0.7
Casson	$K = 0.75, \tau_0 = 3.0$	0.09	1.33

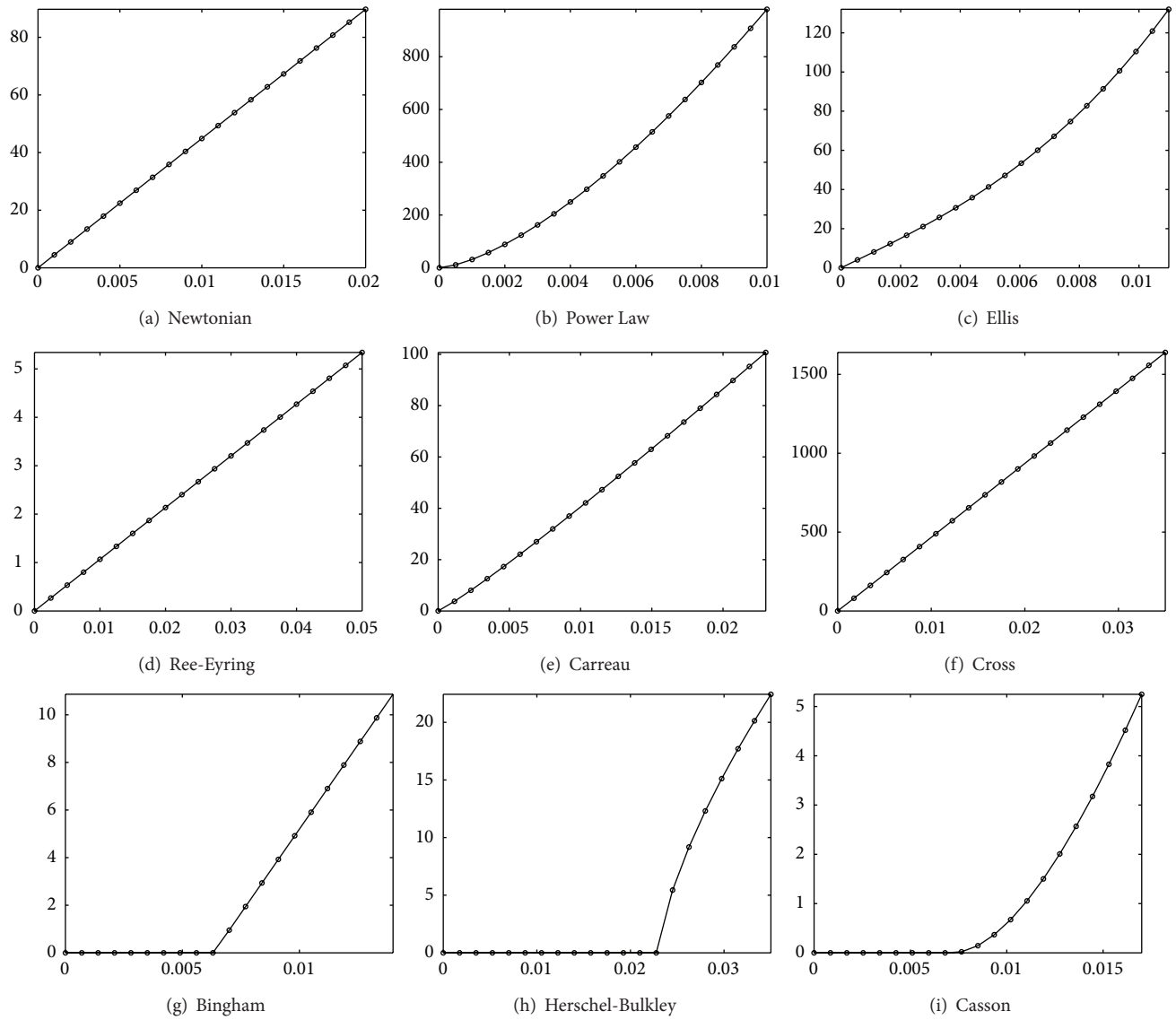

Figure 4: Comparing the analytical solution (solid line) to the variational solutions (circles) of γ in s^{-1} (vertical axis) versus z in m (horizontal axis) for the flow of the nine fluid models in slits. The EL solutions are not represented for the Ellis and viscoplastic fluids. The slit and fluid parameters are given in Table 5, where in all cases $\Delta p = 700$ Pa.

Table 5: Fluid and slit parameters for the examples of Figures 4 and 6, where in all cases $W = 1.0$ m. SI units apply to all dimensional quantities as given in Nomenclature.

Model	Fluid properties	B	L
Newtonian	$\mu_o = 0.13$	0.02	1.2
Power Law	$k = 0.073, n = 0.67$	0.01	0.95
Ellis	$\mu_e = 0.049, \tau_h = 5.0, \alpha = 2.9$	0.011	1.95
Ree-Eyring	$\mu_r = 0.57, \tau_c = 75$	0.05	11.5
Carreau	$\mu_0 = 0.32, \mu_i = 0.096, \lambda = 0.75, n = 0.85$	0.023	0.75
Cross	$\mu_0 = 0.015, \mu_i = 0.007, \lambda = 2.56, m = 0.73$	0.035	2.13
Bingham	$C' = 0.48, \tau_0 = 4.3$	0.014	1.03
Herschel-Bulkley	$C = 0.03, \tau_0 = 5.2, n = 1.45$	0.035	3.09
Casson	$K = 0.12, \tau_0 = 2.15$	0.017	2.33

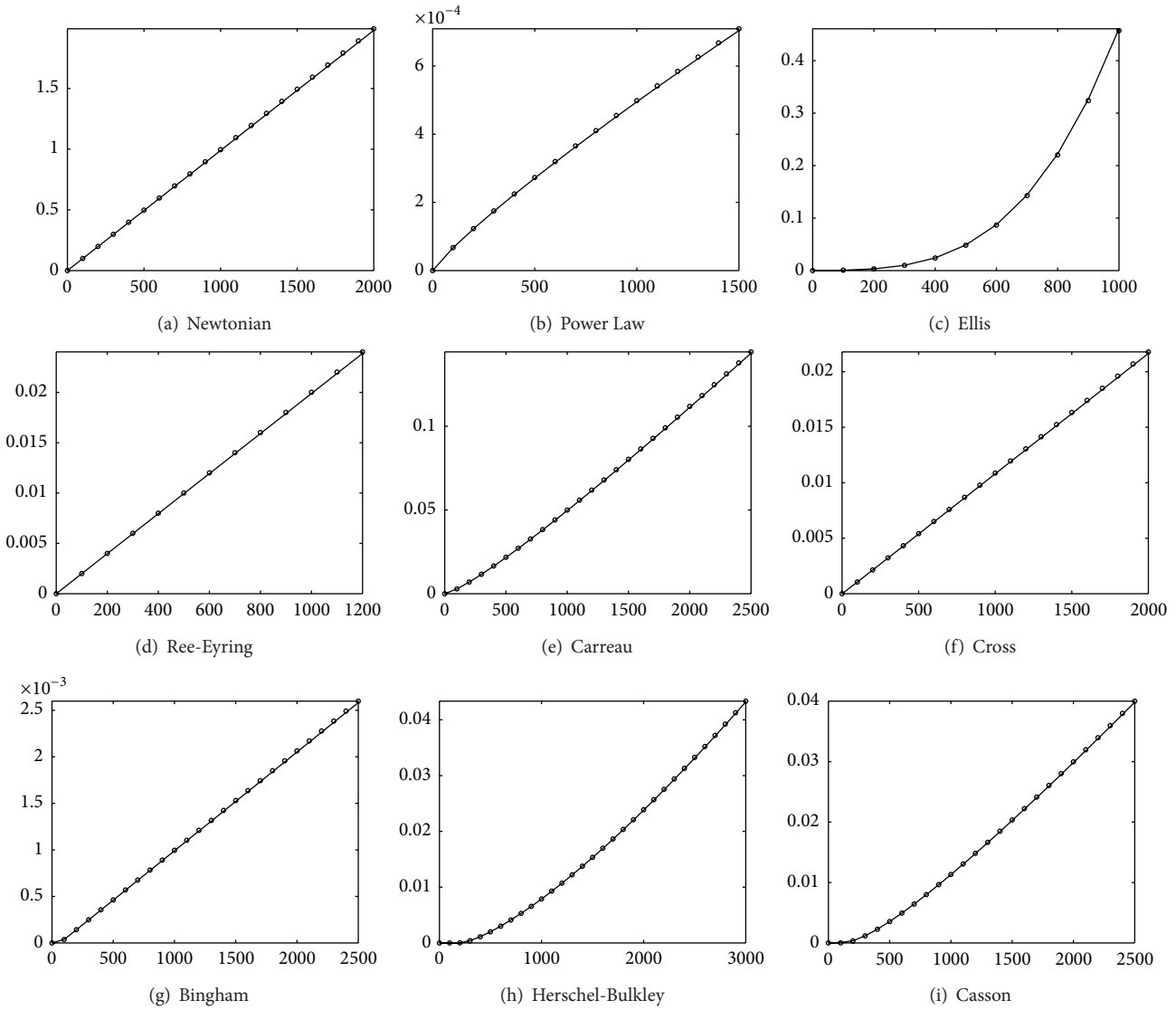

Figure 5: Comparing the analytical solution (solid line) to the variational solutions (circles) of Q in $m^3 \cdot s^{-1}$ (vertical axis) versus Δp in Pa (horizontal axis) for the flow of the nine fluid models in pipes. The EL solutions are not represented for the Ellis and viscoplastic fluids. The pipe and fluid parameters are given in Table 4.

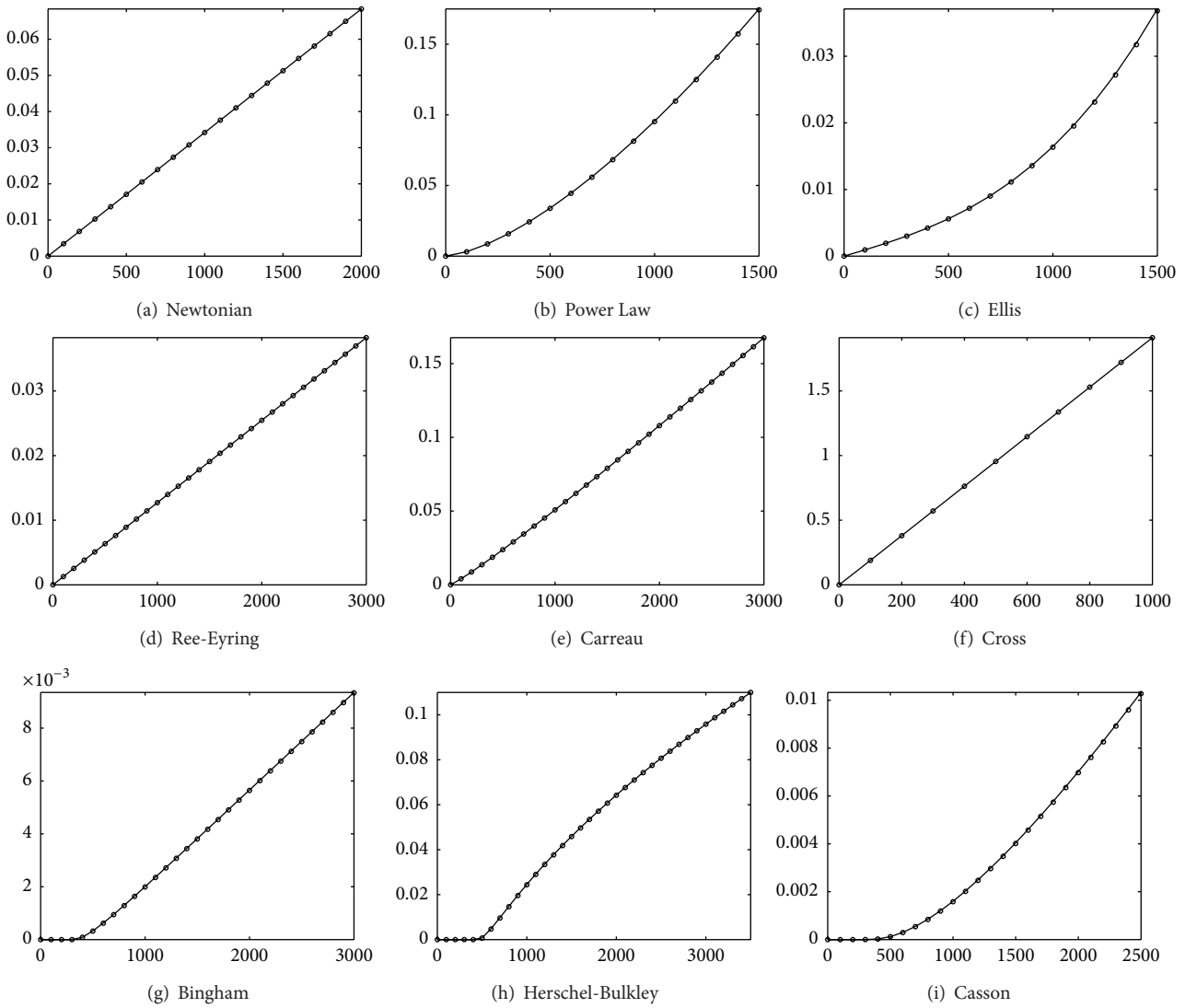

Figure 6: Comparing the analytical solution (solid line) to the variational solutions (circles) of Q in $m^3 \cdot s^{-1}$ (vertical axis) versus Δp in Pa (horizontal axis) for the flow of the nine fluid models in slits. The EL solutions are not represented for the Ellis and viscoplastic fluids. The slit and fluid parameters are given in Table 5.

solutions that other methods might fail to provide or the DM method may require less effort to obtain the solutions than the effort required by the other methods.

Nomenclature

α: Indicial parameter in Ellis model
γ: Rate of shear strain (s^{-1})
γ_B: Rate of shear strain at slit wall (s^{-1})
γ_R: Rate of shear strain at pipe wall (s^{-1})
γ_w: Rate of shear strain at conduit wall (s^{-1})
δ: $\mu_0 - \mu_i$ (Pa·s)
λ: Characteristic time constant in Carreau and Cross models (s)
μ: Fluid shear viscosity (Pa·s)
μ_0: Zero-shear viscosity in Carreau and Cross models (Pa·s)
μ_e: Low-shear viscosity in Ellis model (Pa·s)
μ_i: Infinite-shear viscosity in Carreau and Cross models (Pa·s)
μ_o: Newtonian viscosity (Pa·s)
μ_r: Characteristic viscosity in Ree-Eyring model (Pa·s)
τ: Shear stress (Pa)
τ_0: Yield stress in Bingham, Herschel-Bulkley, and Casson models (Pa)
τ_B: Shear stress at slit wall (Pa)
τ_c: Characteristic shear stress in Ree-Eyring model (Pa)
τ_h: Shear stress when viscosity equals $\mu_e/2$ in Ellis model (Pa)
τ_m: Shear stress at conduit center (Pa)
τ_R: Shear stress at pipe wall (Pa)
τ_w: Shear stress at conduit wall (Pa)

Ω: Spatial domain in Dirichlet functional (m)
B: Slit half thickness (m)
C: Viscosity coefficient in Herschel-Bulkley model (Pa·s^n)
C': Viscosity coefficient in Bingham model (Pa·s)
D: Dirichlet functional (Pa^2·m^{-1})
f: $\lambda^m \gamma_w^m$
${}_2F_1$: Hypergeometric function
g: $1 + f$
G: Constant in the reduced momentum equation (Pa·m^{-1})
$I_{p,Ca}$: Definite integral for Carreau model pipe flow (Pa^3·s^{-1})
$I_{p,Cr}$: Definite integral for Cross model pipe flow (Pa^3·s^{-1})
$I_{s,Ca}$: Definite integral for Carreau model slit flow (Pa^2·s^{-1})
$I_{s,Cr}$: Definite integral for Cross model slit flow (Pa^2·s^{-1})
k: Viscosity coefficient in Power Law model (Pa·s^n)
K: Viscosity coefficient in Casson model (Pa·s)
L: Conduit length (m)
m: Indicial parameter in Cross model
n: Flow behavior index in Power Law, Carreau, and Herschel-Bulkley models
Δp: Pressure drop across conduit length (Pa)
Q: Volumetric flow rate (m^3·s^{-1})
r: Radius (m)
R: Pipe radius (m)
s: Spatial coordinate representing r for pipe and z for slit (m)
T: Stress domain in Dirichlet functional (Pa)
v: Fluid speed in the flow direction (m·s^{-1})
W: Slit width (m)
z: Spatial coordinate of slit thickness (m)
DM: Variational method based on applying Dirichlet principle
EL: Variational method based on applying Euler-Lagrange principle.

Conflict of Interests

The author declares that there is no conflict of interests regarding the publication of this paper.

References

[1] D. R. Willis, "Mass flow through a circular orifice and a two-dimensional slit at high Knudsen numbers," *Journal of Fluid Mechanics*, vol. 21, no. 1, pp. 21–31, 1965.

[2] N. Aksel, "Pressure-induced compressible Newtonian flow in a slit," *Applied Scientific Research*, vol. 45, no. 1, pp. 3–16, 1988.

[3] R. J. Mannheimer, "Laminar and turbulent flow of cement slurries in large diameter pipe: a comparison with laboratory viscometers," *Journal of Rheology*, vol. 35, no. 1, pp. 113–133, 1991.

[4] J. Billingham and J. W. J. Ferguson, "Laminar, unidirectional flow of a thixotropic fluid in a circular pipe," *Journal of Non-Newtonian Fluid Mechanics*, vol. 47, pp. 21–55, 1993.

[5] M. P. Escudier and F. Presti, "Pipe flow of a thixotropic liquid," *Journal of Non-Newtonian Fluid Mechanics*, vol. 62, no. 2, pp. 291–306, 1996.

[6] R. T. Steller, "Generalized slit flow of an Ellis fluid," *Polymer Engineering & Science*, vol. 41, no. 11, pp. 1859–1870, 2001.

[7] P. J. Oliveira, "An exact solution for tube and slit flow of a FENE-P fluid," *Acta Mechanica*, vol. 158, no. 3-4, pp. 157–167, 2002.

[8] M. F. Letelier and D. A. Siginer, "On the flow of a class of viscoinelastic-viscoplastic fluids in tubes of non-circular contour," *International Journal of Engineering Science*, vol. 45, no. 11, pp. 873–881, 2007.

[9] W. L. Barth, L. V. Branets, and G. F. Carey, "Non-Newtonian flow in branched pipes and artery models," *International Journal for Numerical Methods in Fluids*, vol. 57, no. 5, pp. 531–553, 2008.

[10] L. Chen, Y. Duan, C. Zhao, and L. Yang, "Rheological behavior and wall slip of concentrated coal water slurry in pipe flows," *Chemical Engineering and Processing: Process Intensification*, vol. 48, no. 7, pp. 1241–1248, 2009.

[11] D. M. Kalyon, "An analytical model for steady coextrusion of viscoplastic fluids in thin slit dies with wall slip," *Polymer Engineering & Science*, vol. 50, no. 4, pp. 652–664, 2010.

[12] R. Ellahi, "The effects of MHD and temperature dependent viscosity on the flow of non-Newtonian nanofluid in a pipe: analytical solutions," *Applied Mathematical Modelling*, vol. 37, no. 3, pp. 1451–1467, 2013.

[13] A. W. Shaikh and G. Q. Memon, "Analytical and numerical solutions of fluid flow filled with and without porous media in circular pipes," *Applied Mathematics and Computation*, vol. 232, pp. 983–999, 2014.

[14] T. Sochi, "Using the Euler-Lagrange variational principle to obtain flow relations for generalized Newtonian fluids," *Rheologica Acta*, vol. 53, no. 1, pp. 15–22, 2014.

[15] T. Sochi, "Further validation to the variational method to obtain flow relations for generalized Newtonian fluids," *Korea-Australia Rheology Journal*, vol. 27, no. 2, pp. 113–124, 2015.

[16] T. Sochi, "Variational approach for the flow of Ree-Eyring and Casson fluids in pipes," http://xxx.tau.ac.il/abs/1412.6209.

[17] T. Sochi, "Analytical solutions for the flow of Carreau and Cross fluids in circular pipes and thin slits," Accepted in *Rheologica Acta*.

[18] T. Sochi, "Slip at fluid-solid interface," *Polymer Reviews*, vol. 51, no. 4, pp. 309–340, 2011.

[19] A. H. P. Skelland, *Non-Newtonian Flow and Heat Transfer*, John Wiley & Sons, New York, NY, USA, 1967.

[20] R. B. Bird, R. C. Armstrong, and O. Hassager, *Dynamics of Polymeric Liquids*, vol. 1, John Wiley & Sons, 2nd edition, 1987.

[21] W. H. Press, S. A. Teukolsky, W. T. Vetterling, and B. P. Flannery, *Numerical Recipes in C++: The Art of Scientific Computing*, Cambridge University Press, Cambridge, UK, 2nd edition, 2002.

[22] C. G. E. Boender, A. H. G. Rinnooy Kan, G. T. Timmer, and L. Stougie, "A stochastic method for global optimization," *Mathematical Programming*, vol. 22, no. 1, pp. 125–140, 1982.

[23] T. Sochi, "Solving the flow fields in conduits and networks using energy minimization principle with simulated annealing," http://arxiv.org/abs/1408.0357.